Design and Development of Low Cost 3D Printed Ambidextrous Robotic Hand Driven by Pneumatic Muscles

Emre Akyürek, Tatiana Kalganova, Mashood Mukhtar, Leonid Paramonov, Luke Steele, Michal Simko, Luke Kavanagh, Alisdair Nimmo, Anthony Huynh, Stelarc

Abstract— This paper presents the mechanical design and development process of an ambidextrous robot hand driven by pneumatic muscles. The ambidextrous hand is capable of performing both right hand and left hand movements. In addition to ambidextrous movements, hand offers a range twice larger than common fingers. The mechanical design of an ambidextrous robot has been investigated in a way to reduce maximum possible number of actuators. Actuated by only 18 pneumatic muscles, the ambidextrous hand has a total of 13 degrees of freedom which permit to imitate equally a hand of each side. The ambidextrous hand is 3D printed after carefully analyzing the material, tendon routing, kinematic performance and overall design parameters. The main application areas of this project are in rehabilitation and physiotherapy after strokes and management of phantom pain for amputees by controlling the robotic prosthesis remotely via internet and social media interface. The ambidextrous feature of the robotic hand allows completing the tele-rehabilitation for both left and right hands using one robotic device.

Index Terms— Robot Hand; Ambidextrous Design; Pneumatic Muscles; Numerical Simulations

I. INTRODUCTION

Human hand is perfectly engineered by nature. It is considered as one of the complicated parts of our body due to its unique and complex movements. A human hand has 27 degrees of freedom [51] which allows a large range of movements and tasks such as grasping variety of objects, adaption, manipulation, perception, prehension and exploration [44].

In human's daily life, almost every task involves use of hand. Each task specifically demands in its own set of requirement to perform it precisely and correctly. In this rapidly growing industrial society some tasks are too risky for human to attempt [56]. The adroitness of human hand to perform such

exceptional tasks resulted in production of number of robotic hands in the last few decades [19]. The hand's dexterity has been recognized and extensively discussed in the field of robotics [45], [46], [47], [48] and [49]. Although a number of dexterous hands have been used in biomedicine area [8] and [9], none of them considered the possibility of an ambidextrous architecture, allowing a significant reduction in the implementation of resources for treatment of phantom limb pain patients. In this paper we present a novel design of low cost 3D printed ambidextrous hand which may be used in future to alleviate phantom limb pain. Various robotic hands have been developed for different purposes in the past are shown in figure 1.
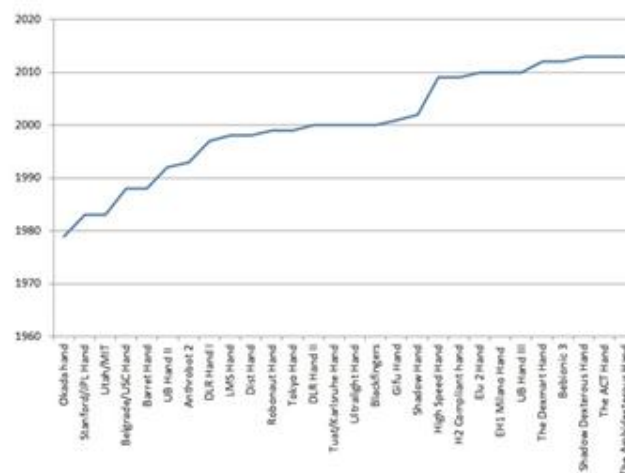

Figure 1: Robotic hands and year of development

Phantom limb pain is a pain experienced by 50-80% amputees in an absent limb [52], [53]. Number of treatments has been used in the past to reduce phantom limb pain namely mirror box therapy and virtual reality [50]. As it has been clinically proven that both mirror boxes [1] and the use of virtual reality [2] contribute to phantom limb pain relief, the control of the ambidextrous hand should contribute to pain relief if its movements are close enough to the ones of a human hand. Amputees or people suffering from neurological disorder have been provided assistance by connecting robot limbs to a brain-machine interface [3], [4] robotic hands have also been used as rehabilitation devices for recovering patients [5], [6]. However, most of rehabilitation devices are expensive [8], [12] or difficult to access in short delays and none of them propose a free therapy treatment instantly accessible online.

To increase this ease of accessibility, the ambidextrous hand can imitate the movements either of a right hand or a left hand

(Figure 2), permitting assistance to injuries of both sides with only one robotic device. Thus, it means fingers can bend totally in one way or another, with a range of motion twice larger than human fingers. The possibility of such a system has been proved in an early stage of this research by connecting the robotic device to a remote-control interface with a video streaming as feedback [7]. This new work focuses on the modeling and the testing of 3D printed mechanical designs to reach such a range of movements and leads to the final design of the ambidextrous robot hand. Comparisons and analysis have been done about the material, the tendons routing configurations and the mechanical designs to obtain optimized ambidextrous features [43].
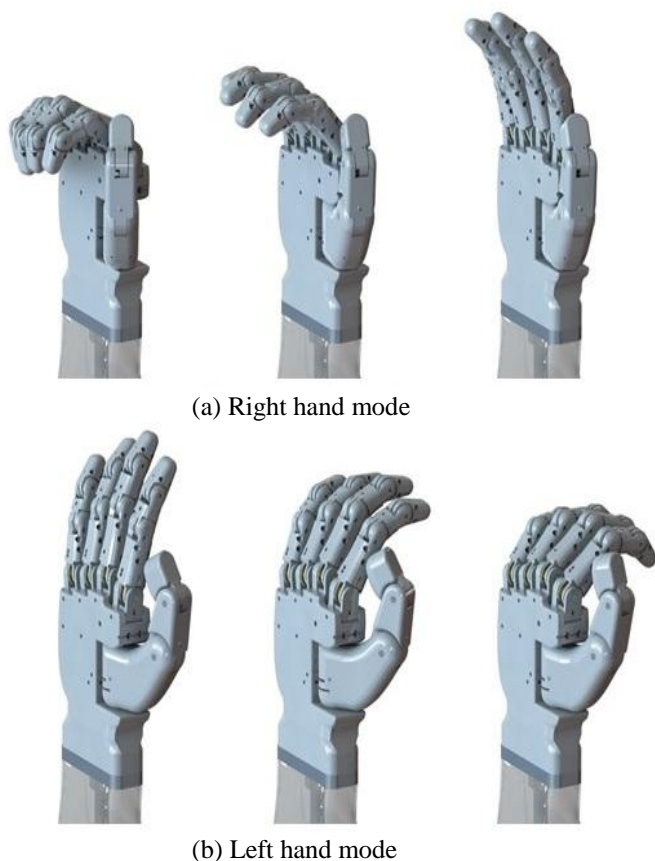

(a) Right hand mode

(b) Left hand mode

Figure 2: Ambidextrous hand from right to left mode

Before proceeding to mechanically design the ambidextrous robot hand, previous models of related research have been analyzed and compared to find the most efficient way of implementation. The literature review is provided in the 'Related Research' section of the paper, with an emphasis on the different actuators usable to drive robot hands. Kinematic features of ambidextrous fingers are investigated in 'Simulation of Numerical Models' section. A number of intermediate manufactured designs, concerning choice of material, tendon routing investigation and maximization of the range are already discussed in great details [43]. Their kinematic performances and the results achieved with each of them are analyzed and compared [43]. Mechanical design section describes how the models are combined into a final unified design. The last sections of the paper concern the design of the thumb and the palm, which include the implementation of abduction and adduction.

II. RELATED RESEARCH

Design of robotic hands should be based on the knowledge of anatomical science so the final product can be manufactured as close as possible to human hand [54] in terms of mechanical structure and functionality. The ACT hand [11] is found to be one of the finest designed built ever. Bionic hand is built specially to transplant on forearm [8]. Some prostheses neither include electronic devices nor have independent motions for fingers [9], [10], which allow them to be low cost in addition to be lightness.

Primarily, Robotic hands are divided into two types; built-in actuator type and external actuator type [55] and there are three ways to actuate a robotic hand; body-powered, controlled by motors or driven by pneumatic artificial muscles (PAMs). Mechanical features of these three kinds of robotic hands are gathered in Table I. Depending on the objectives of the designers, the main specifications can be totally different from one hand to another.
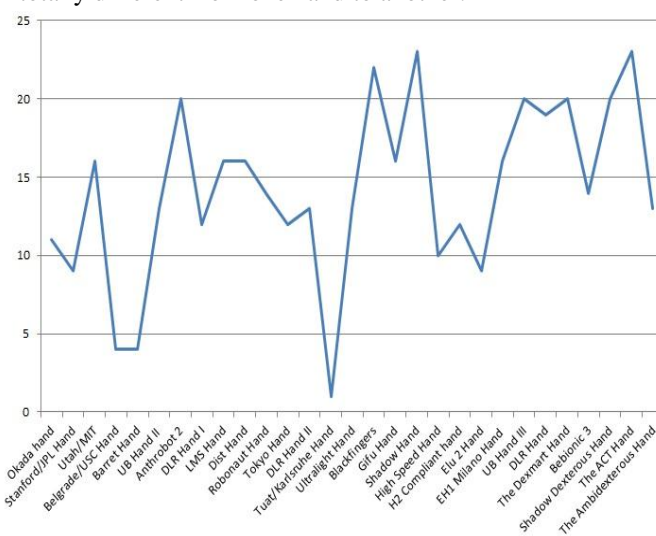

Figure 3: Various robot hand vs degree of freedom

In the realm of robot hands, the main objective was to control as many degrees of freedom (DOFs) as possible and to reach behaviour close to a human hand [11], [12], [13], [14]. Figure 3 shows the various hands developed in the past and their degree of freedom. It is noted from the figure 3 that degree of freedom on average has increased by the passage of time. Although much work was done to build robotic hands with maximum possible degree of freedom but some institution opt for a high-speed control [15], far faster than a human hand, even if it implies to reduce the number of fingers to reach such accuracy [16]. For other structures, designers found a compromise between the number of actuators and the DOFs to have a good control of the hand with fewer resources [17]. Such results can be obtained with an optimized architecture, although some joints are not controlled independently [18].

It is noticed that most of dexterous robotic hands are controlled by motors instead of PAMs [19]. This is due to the existence of non-linearity between the contraction of the PAM and the provided force [20], [21], which makes it difficult to control the hand properly. However, PAMs permit extra flexibility to the overall behaviour of the system [22], and some institutions have proved that it is possible to drive efficiently robotic hands using this technology [23], [14].

Comparing the numbers of actuators, it can be observed that PAMs are generally almost twice numerous than motors to command as many DOFs. Some hands successfully reduced this ratio by implementing directly the muscles inside the fingers' architecture [14], [22], [24].

As no ambidextrous designs have been found in the literature review, numerical models have been simulated to investigate different kinematic features and to analyze different geometric structures. The aim was to prove numerically the ambidextrous concept before designing the first prototypes.

Robotic Hands	Mechanical features				
	# and kind of actuators	# fingers	# DOFs	Range of motion	Speed of motion
Bionic/Prosthetics					
The SDM Hand [10]	1 motor or body-powered	4	8	< human hand	~ human hand
The Natural Dexterous Hand [9]	1 human shoulder	5	14	< human hand	~ human hand
Bebionic3 [8]	EMG signals, N/A (motors)	5	~14	< human hand	~ human hand
Motor actuated					
Robonaut hand [28]	14 DC motors	5	14	~ human hand	< human hand
S. Kawamura et al. [29]	7 D.C. motors	3	6	< human hand	> human hand
The Southampton remedy hand [17]	6 motors	5	6	< human hand	~ human hand
The Gifu hand III [15]	19 DC servomotors	5	16	~ human hand	1.35× human hand
H. Hu et al. [30]	13 DC motors	4	13	~ human hand	~ human hand
I. Yamano and T. Maeno [31]	~20 ultrasonic motors	5	20	~ human hand	~ human hand
G. Stellin et al. [18]	9 DC motors	5	20	~ human hand	N/A
High-speed hand [16]	N/A motors	3	10	> human hand	>> human hand
H2 Compliant hand [32]	5 motors	4	12	~ human hand	~ human hand
C. Kuo and C. Chen [33]	12 DC servo motors	5	16	~ human hand	N/A
Elu2 Hand [34]	N/A (servomotors)	5	9	~ human hand	~ human hand
The EH1 Milano hand [35]	12 DC motors	5	16	~ human hand	0.12 × human hand
The DEXMART Hand [13]	~20 DC motors	5	~20	~ human hand	~ human hand
DLR hand [25]	42 motors	5	19	> human hand	~ human hand
The Shadow Dexterous hand E1M3R, E1M3L [12]	20 motors	5	20	~ human hand	0.36 × human hand
The ACT Hand [11]	36 DC motors	5	23	~ human hand	~ human hand
Pneumatically actuated					
J. Sancho-Bru et al [24]	25 PAMs	4	20	~ human hand	N/A
D. Wilkinson et al. [36]	31 PAMs	5	~20	~ human hand	N/A
Y. Honda et al, 2010 [22]	25 PAMs	5	17	~ human hand	N/A
The ExoHand [14]	26 PAMs	5	~ 20	~ human hand	~ human hand
The Shadow Dexterous Hand E1P1R, E1P1L [23]	40 PAMs	5	20	~ human hand	0.5 × human hand
Ambidextrous hand (proposed, 2013)	18 PAMs	5	13	> human hand	> human hand

TABLE I: CLASSIFICATION OF DIFFERENT ROBOTIC HANDS' FEATURE

When the fingers' tendon routing is showed, it is seen that an important number of PAMs is necessary only to control the flexion/extension. Four PAMs are used for this purpose in [22].

The second main objective of the ambidextrous robot hand is to investigate several tendon routings precisely to minimize the number of PAMs. It is noted that some other robotic hands include more actuators than necessary to reach new kind of behaviours, such as compliancy [11] or robustness [25].

III. SIMULATION OF NUMERICAL MODELS

A numerical model for testing different types of tendon routing was created in Matlab/Python. The main purpose of the model was to investigate basic properties of planar tendon systems for actuation of an ambidextrous finger within the ambidextrous hand project. The model was used to investigate behaviour of the potential ambidextrous finger designs being actuated by PAMs. The model can be used for investigation of planar tendon driven mechanisms being actuated by any type of actuators given the model of the actuator is added to the package.

It is assumed that the ambidextrous finger design consists

of a number of rigid bodies connected via cylindrical revolute joints with parallel axis. It was also initially assumed that the whole kinematic structure can be represented by a tree graph without loops. The kinematic structure of the finger is being actuated by tendons/strings running over a number of pulleys attached to the rigid bodies via frictionless cylindrical revolute joints. Also an assumption was made that the tendons themselves are transferring the tension load to the pulleys without losses due to elastic and friction forces. This assumption was made due to the fact that the tendon material is much more rigid under tensile loads than the PAMs, which are changing their elasticity and length depending on the pressure of the gas inside and the current length [26], [27]. This assumption can be later removed by developing the tendon model further if experiment show importance of tendon elasticity.

An important feature of the model which allowed investigation of ambidextrous finger designs was ability of the tendon strings to lift off and touch back down to the pulleys. It was important for ambidextrous function because the same tendons had to work in contractor and extender modes depending on the direction of the operation. The main difficulty in developing of the model development was design of an algorithm which was able to resolve changing geometric structure of the tendon interaction with pulleys due to tendon not being in contact with some of the pulleys.

In such form the library can be used to simulate geometric characteristics of a given tendon driven mechanism but such simulation is pretty much limited to calculation of variation of the length of all tendons included in the design. To allow for simulation of static forces acting on the mechanical structure due to forces produced by PAMs a quadratic potential function was assigned due to variation of length of each tendon. A static equilibrium of the mechanical structure of a given finger design can be then found by minimizing the total potential energy of all tendons in the system. This simple elastic model will be later replaced with a model of PAM based on experiments.

The static mechanical model based on minimization of the total potential energy of the mechanism allowed for straightforward introduction of a simple elastic contact model based on penetration distance of pairs of rigid bodies. The contact forces due to the elastic contacts introduced this way were treated as external forces applied to the mechanical structure of the finger. The elastic constant of the contact forces was kept one or two orders of magnitude higher than the elastic constant of the tendon potential function to represent difference between "soft" and "stiff" elements of the finger design. The introduction of contact forces allowed for investigation of efficiency of the various finger designs in few grasping scenarios.

The model was first developed in Matlab. An XML based format was used for input/output of model parameters definition. Later the library was rewritten in Python which allowed adding higher flexibility for usage of the library in different control scenarios. Once satisfactory behaviours were obtained with numerical models, similar ones have been manufactured.

IV. MECHANICAL DESIGN

In order to imitate behaviour of a finger, maximum of its degrees of freedom (DOFs) must be reproduced. Human fingers can make two kinds of antagonist movements: flexion and extension, or abduction and adduction. Flexion and extension control the angular displacement of the three phalanges of a finger, which means as many DOFs. Abduction and adduction imply lateral rotations of a whole finger and constitute another DOF, which makes a total of four distinct DOFs per finger [37]. As abduction and adduction are not essential for a number of applications, a number of dexterous hands have been developed without taking them into account [34], [32], [38]. It allows both easing the control of the structure and reducing the number of needed actuators. As the movement of both distal and medial phalanges is coupled together in case of the human hand, these DOFs are often controlled by a single actuator [12], [13]. In these cases, the flexion/extension of the proximal phalange is driven by a second actuator while the finger's abduction/adduction is controlled by a third one. Robot fingers are usually built as a succession of three phalanges, with sockets preventing them to reach non-natural angles [31], [39]. These sockets must be ignored to reach the range necessary to ambidextrous fingers, which is twice larger than the one of common fingers. Besides, as the ambidextrous fingers are controlled with PAMs, to reach their two extreme positions is the main difficulty of the research. Indeed, the two main kinematic features to take into account are the stretching force of the antagonist PAM, which provides a huge force cancellation when the first PAM is contracting and the limitation of the PAM extension. Consequently mechanical designs have to be optimized according to the PAM's elasticity, taking into account both their active and passive ranges. It is noted that these issues do not occur with motorized fingers, so PAMs can be replaced by servomotors motors for further research.

Another issue to be considered is the number of PAMs necessary to control one finger. The antagonist movements are often simulated with PAMs used by pairs [40], [22], [41], which means that the system would require twice more PAMs as DOFs, even though a minimum number of $n+1$ actuators is necessary to control a number of n DOFs [29]. To have a compromise between an efficient dexterity and a limited number of muscles, tests were done both with four and three muscles to control the flexion/extension of a single finger. To proceed forward, four main models focusing on different aspects have been designed on CAD software, analyzed on Matlab and manufactured for testing purposes. The experiments were done on the test bench shown in figure 4.

The prototypes were connected to position sensors, pressure transducers and load cells. The aim was to cover as many as worth considering solutions as possible and to use the collection of experimental data to analyze their kinematic behaviors.

The first prototype mainly aimed to validate the choice of the material and to consider the reduction of the friction. The second one was used to test many different tendon configurations and multiple sizes of pulleys. Experiments were also done to confirm that it was possible to drive an ambidextrous finger with three PAMs. The third prototype kept going on this way, with the use of offset pulleys to benefit of the maximum of the muscles' range. The fourth model was designed with accurate geometrical features in the aim of rectifying the imperfections of previous designs. The more

efficient solutions were combined to design a final version of an ambidextrous finger.
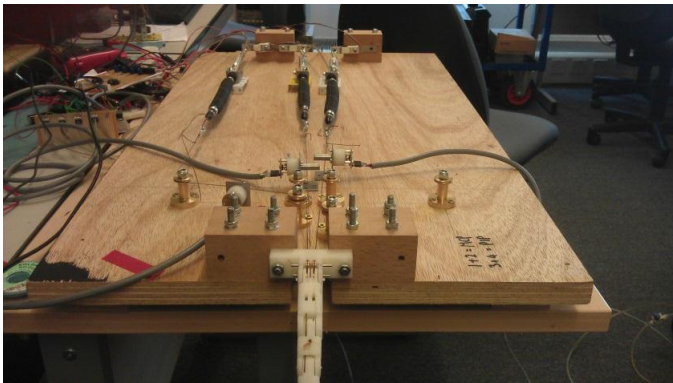

Figure 4: Test bench with a prototype attached to PAMs and sensors

A. Unified finger design

After initial testing to establish the kinematic ranges of the fingers [43], it was decided to proceed with an implementation of the three tendons routing schemes, implementing the offset pulleys in the medial phalanx base, but utilizing bearing-based joints. An additional aim is to implement a bearing-based joints and a similar spiral or offset pulley for the base of the proximal phalanx, with the intention of maximizing compression torque but minimizing the spring force of the muscle at the opposite extreme of motion.

The tendon scheme is a variation of the three tendons routing method. The primary differences are in the use of offset pulleys at pulley location c. In addition, incorporation of pulley b into the proximal phalanx allows the use of spiral, offset circular and uniform circular forms for that pulley. The overall routing scheme is illustrated in Figure 5.

The pulley b is shown in figure 6. It can be seen it incorporates a bigger diameter when the muscle contracts and a smaller diameter when the muscle is in passive extension. It reduces the extension of the muscle, which makes the opposing force lower.

Another substantial requirement for the final finger prototype is to incorporate position sensing in the phalanx joints. It is also considered desirable to investigate the possibility of building the design parametrically in order that customized phalanx lengths for all four fingers could be implemented.
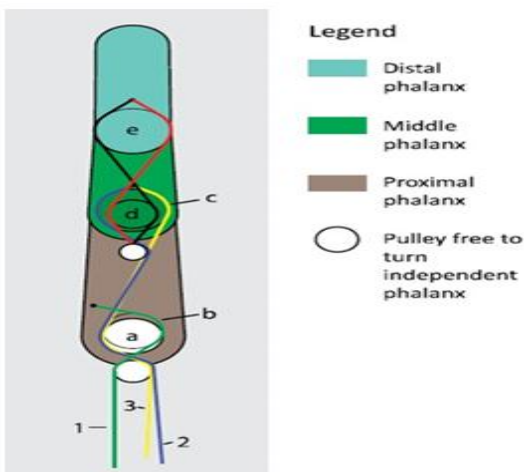

Figure 5: Finalized tendon routing scheme

Consequently, the second main goal of the design is to accommodate the position sensor assembly within the joint without significantly increasing thickness or reducing joint strength. Figure 7 shows the adapted proximal / knuckle joint designed for this purpose.
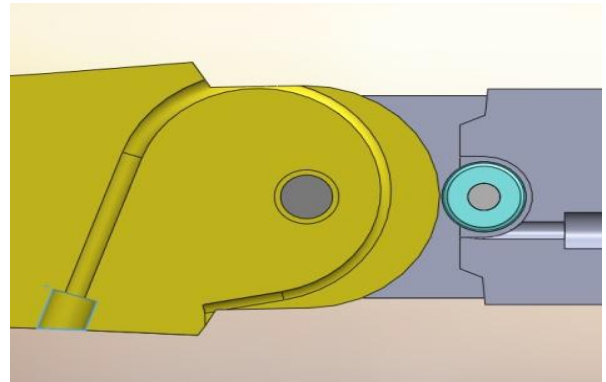

Figure 6: Offset circular pulley b

The axle (dark grey) is 4mm in diameter with an enlarged 6mm diameter boss at one end which butts up against the magnet (white) – the boss and magnet are both held concentric within a 6x10x2.5mm bearing (green). The lower side of the boss - facing the 4mm part of the shaft - butts up against the proximal phalanx body. The 6x10x2.5mm bearing is held in a recess in the knuckle. The other end of the axle is held in a 4x7x2.5mm bearing, which in turn sits in a suitably sized recess in the knuckle.
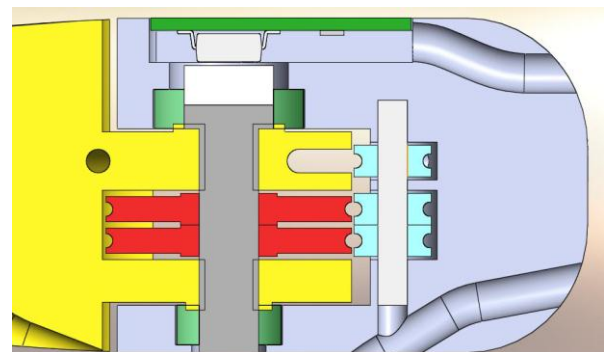

Figure 7: Joint design

The proximal phalanx (yellow) features bosses to ensure the phalanx is in contact only with inner races of the bearings – the outer races sit in contact with the knuckle. Pulley b is integrated into the surface of the proximal phalanx. The two a pulleys (red) are machined from brass with a loose sliding fit to ensure free rotation on the axle. All three peripheral pulleys (cyan) sit on the same axis in the knuckle. The proximal/knuckle axle sits in the proximal phalanx with a tight fit – hence the axle, 6x10x2.5mm inner bearing recess and magnet rotate together. The recess in the knuckle immediately above the bearing ensures the magnet does not foul on the knuckle. The sensor board is held by a second recess, retained by friction fit with the ABS surface (Figure 8).

The proximal / medial joint is shown in figure 9 and is formed around a 3mm axle (dark grey) machined from mild steel, constrained by two bearings (green). The axle is held by friction fit to ensure rotation with the medial phalanx. The top of the axle features an enlarged (6mm diameter) boss that sits against the inner race of the upper bearing.
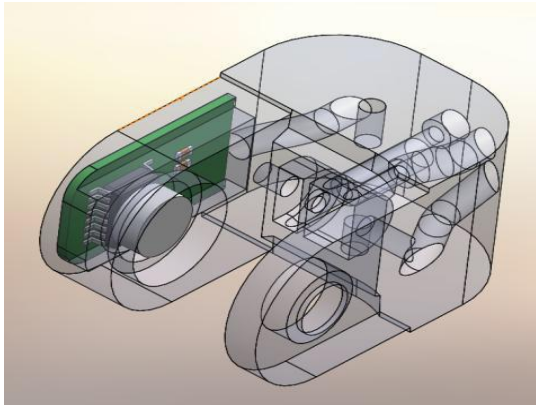
Figure 8: Sensor assembly in the knuckle

The magnet (white) is attached to the axle boss with fast drying epoxy, to provide sufficient curing time to be able to ensure concentricity. The proximal phalanx contains a recess to provide sufficient clearance for the magnet. The sensor assembly is retained in place by friction fit, and can be glued in place after assembly. The tendon #2 reversal pulley (cyan) sits on a 2mm silver steel axle located inside the proximal phalanx. The joint utilizes the same overlapping pulley scheme, the main difference however is that the tendon planes are slightly offset laterally to allow for the c pulley axis to be offset and avoid them to intrude into the d pulley area.

The medial / distal joint is showed in figure 10 and utilizes a 3mm shaft constructed from silver steel, mounted in two 3x6x2.5mm bearings. These bearings are held within the distal phalanx (grey), due to its greater thickness. The lower groove in which the coupling tendon runs in the distal phalanx is
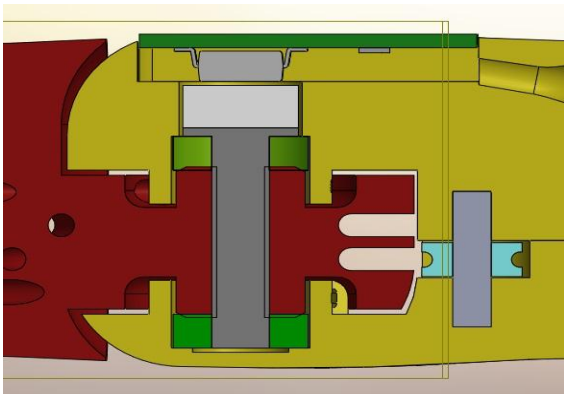

Figure 9: Proximal/medium joint

displaced significantly to one side as a consequence of the asymmetry of the proximal / medial joint, causing the two tabs of the medial phalanx (yellow) which form the joint to be comparatively thin (approximately 3mm). The final dimensions of the fingers are provided in Table II.

In addition to angular position, the implementation of a tactile system is necessary to permit the ambidextrous hand to grab objects. Two kinds of sensors were connected to the prototypes during experiments: load cells, at the base of PAMs, and pressure transducers, directly receiving inputs from the pneumatic circuit.
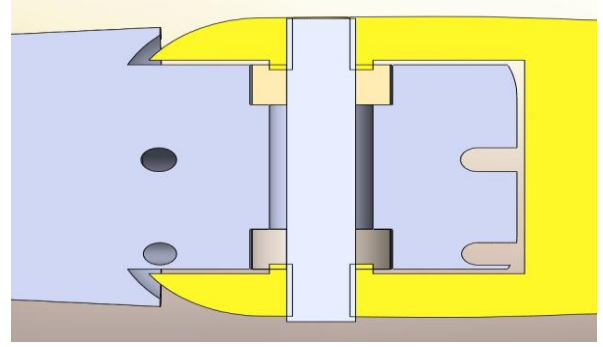

Figure 10: Medial/distal joint

Experimental data was collected based on angular feedback. The ambidextrous finger has a total of three extreme positions by phalanx (or coupled phalanx) that are straight, right or left, which means a total of nine extreme positions for the whole structure. The experiments were done reaching each of them to cover the whole range of movements. The measurement of both force and pressure from the PAM directly connected to the proximal phalange are indicated in figure 11. The angle of the proximal joint is also included in the diagram, while the medial / distal phalanges were also rotating between their extreme positions. It is seen that force and pressure behaviors are very close and, as similar results are obtained with the two other PAMs, the force feedback can be adequately generated from the pressure transducers, as the implementation of load cells would complicate the design of the forearm.

The next section of this paper concerns the thumb, easier to implement because its ambidextrous feature only concerns a wider range around its rotational axe.

V. THUMB

The thumb is designed symmetrically around a plane midway between the palm and dorsal surfaces (between both palms in the case of the ambidextrous hand) to allow equal movements in both right and left hand modes. Pure extension/flexion of the metacarpal is limited to around 10° in the human hand so the thumb's movement is imitated by making it rotate around a fixed point to produce the required ambidexterity. The design of the thumb is illustrated on figure 12. The metacarpal joint includes two 5x16x5 press fit ball bearings housed inside the metacarpal joint to preserve space in the palm, to minimize friction during adduction and abduction. The bearings act as the load bearing points between the thumb and the palm. Space for centralized tendon routing through and out of the metacarpal is provided by two blind pins that do not connect through the metacarpal. The extension motion of the distal and proximal phalanxes is provided by spring return.

	Proximal	**Medial**	**Distal**
Index	49 mm	25 mm	19.5 mm
Middle	50 mm	30 mm	22 mm
Ring	47 mm	29 mm	19.5 mm
Little	37 mm	21 mm	18.5 mm

TABLE II: PHALANX LENGTHS OF UNIFIED DESIGN

This is made possible by the approach to ambidexterity taken in the thumb where the flexion angle faces in towards the angle of rotation between left and right handed modes through the full range of adduction/abduction, which provides the ambidexterity of the thumb. The metacarpal joint is designed to swing around a fixed axis in the palm in-between the middle and index fingers, and the actuation is provided by an arrangement of two antagonistic tendon muscles paired together. The thumb pad faces the side of the fingers when the metacarpal is in the neutral position.
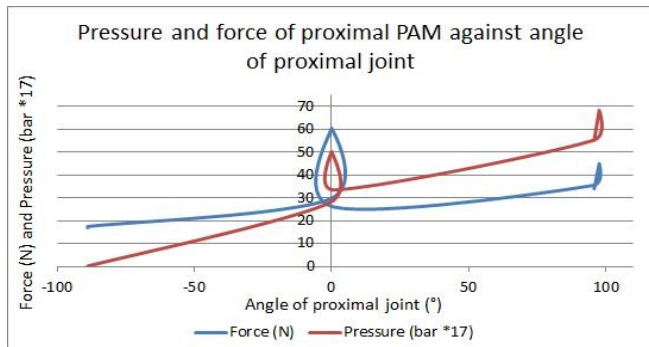

Figure 11: Feedbacks generated from force and pressure sensors while the ambidextrous finger is moving to its different positions

The tendon routing, shown on figure 13, is selected to be as close to the axis of rotation as possible in to reduce any extension of the proximal tendon during adduction/abduction. It is achieved through a single pulley centered on the point of rotation of the thumb. The metacarpal phalanx is simplified to a single DOF system with motion around a single axis in the palm in line with the neutral finger position. The proximal tendon enters the thumb horizontally from the palm and is routed through the center of axis of rotation of the metacarpal joint to negate any extension of the tendon during adduction / abduction of the thumb. A single press-fit silver steel pin is inserted into the metacarpal joint to form a stationary pulley about which the tendon is routed up through the main body of the metacarpal phalanx. A silver steel pulley is used to provide a low friction point of rotation without removing additional material to accommodate a freely rotating pulley and to enhance the stiffness of the thumb.

As the whole five fingers were designed and ready to assemble, the only missing part to achieve an ambidextrous robot hand was the palm.
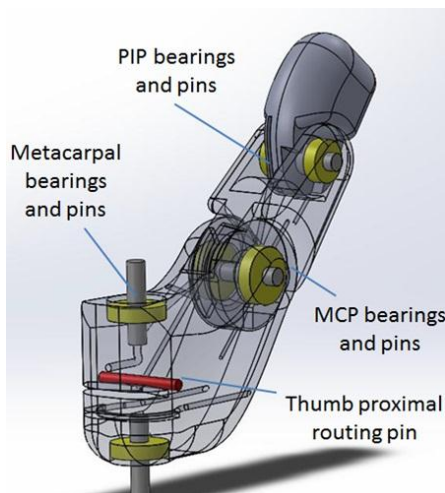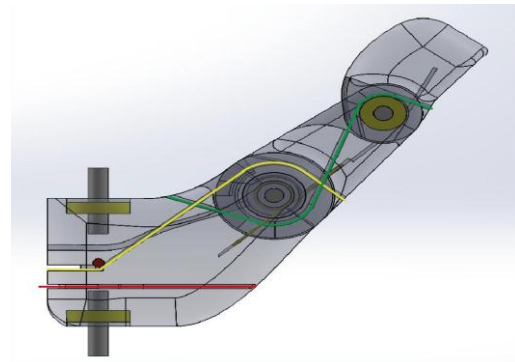

Figure 12: Thumb bearings and pins

Figure 13: Tendon routing in the thumb

VI. PALM

The palm is created as a solid rapid prototyping piece for strength, rigidity and to ensure alignment of the thumb axis. It is essentially formed of two plate-like dorsal and palmar surfaces that are joined by two structural pillars. One is located below the little finger and the second forms a c-shaped structure around the thumb (figure 14). A tendon routing plane is inserted horizontally across the cavity within the palm. Its functions are tendon organization and provision of lateral stability. Knuckle mounting points are offset to mimic the natural geometry of the hand. Bearings are set into the thickness of the palm to carry load radially from the fingers.

The index finger abduction tendon is routed through the thumb support pillar and then over silver steel insert before attaching to the index knuckle (figure 15). Adduction is spring actuated with two 9.5mm extension springs returning the finger. The springs are attached to a thin rod that sits in a recess in the palm and attaches to the bottom of the knuckle. Clearance cut outs for the springs allow the spring to rotate about the rod and the palm thickness around the rod is bolstered to increase reliability.
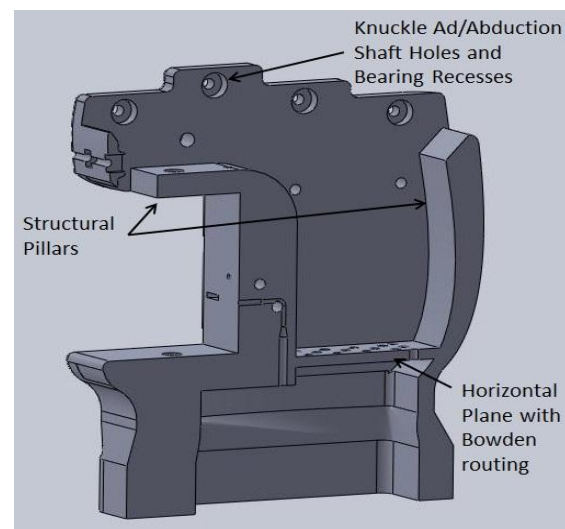

Figure.14: Mid-Plane Frontal Section of Palm to show inner routings and structural pillars.

Abduction of the ring and little finger is achieved in a similar fashion with a tendon routed over a silver steel shaft.

However, the tendon is inserted into the center of a link that joins the two. The ring and little finger have coupled movement to reduce the number of muscles required. Adduction is again dealt with by extension springs attached to a silver steel shaft, inserting onto a small rod that passes through the center of the link. In order to obtain abduction of the ring/little finger that complies with the product design specification, differential rotation was required to match with the 35° angle of little finger and the 25° angle degree of ring finger abductions (figure 16).

$$ratio\ of\ angle = \alpha = 25/35 = 0.714 \qquad (1)$$

$b = 10\ mm$, the distance from the fulcrum to the link pivot point for the little finger. When the little finger is at its fully abducted position:

$$a = \tan(35) * 10 = 7mm = a' \qquad (2)$$

Using a straight link to join the ring and little finger swing arms, the difference in angle becomes a function of the vertical offset between the two fulcrums and can be described as:

$$0.714 = \tan^{-1}\frac{7}{b'} / \tan^{-1}\frac{7}{10} \qquad (3)$$

$b' = 15\ mm$ meaning that the vertical offset, between the little and ring finger fulcrum must be $b'-b = 10\ mm$ to obtain the angle ratio required.

Three tendons route to the thumb, one for flexion of the distal and proximal phalanxes and two for the rotation/swinging movement of the thumb. All routing is dealt with inside the structural thumb pillar for tidiness. All three routes vertically through Bowden cables before exiting over silver steel insert. Bowden cables were utilized to simplify internal tendon routings and avoid unwanted tendon travel during ad/abduction.
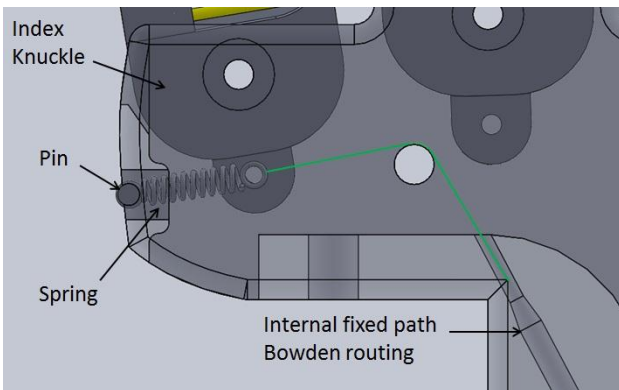

Figure 15: Index finger Ad/Abduction

Thumb ad/abduction tendons are routed over vertical and horizontal shafts, the latter ensuring zero tendon lift at full rotation (figure 17). Press fit silver steel inserts are chosen over pulleys throughout as they offer a better finish than hand turned brass pulleys. The fingers are held to the palm via the knuckle which is attached at the ad/abduction pivot point below the top of the palm.
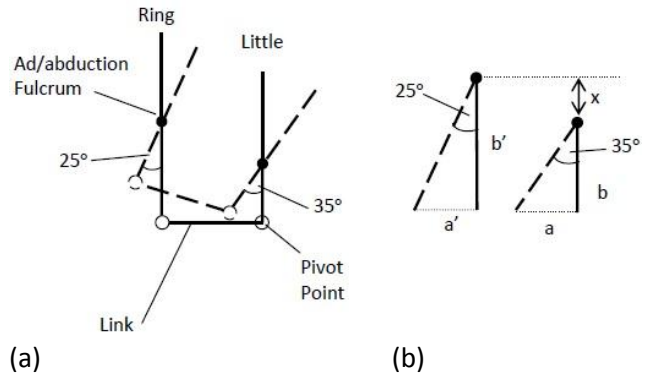

Figure 16: Ring and little fingers abduction, (a) represents the fingers position and (b) introduces the symbols used in (6) and (7)
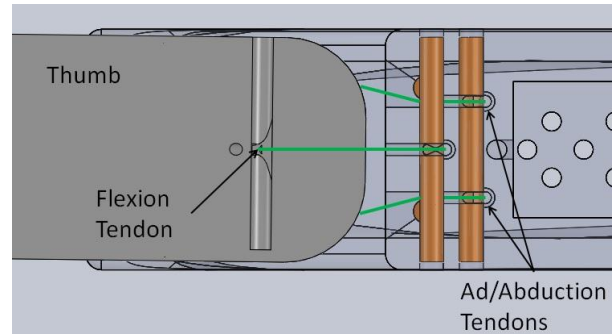

Figure 17: Top view of thumb tendon routing

With this final part of the project designed and manufactured, the different components of the ambidextrous robot hand could be 3D printed and assembled.

VII. CONCLUSION

Starting with the exploration of concept designs for an ambidextrous finger [43], the project moved forward to develop a unified finger design after careful concept evaluation. The full ambidextrous robotic hand with a total of thirteen DOFs controlled by eighteen PAMs was achieved with the design of thumb, palm and forearm. Three tendons, two degrees of freedom prototype fingers were manufactured by rapid prototyping ABS. Refined concepts displayed a full range of motion within design specifications. Difficulties were found concerning pneumatic muscle behavior and ranges, but solutions have been identified and presented, and the final design offers complete kinematic performance. Force and angle feedback were incorporated into the designs to facilitate development for the hand control system. Simple postures of the ambidextrous hand can be seen on figure 18.
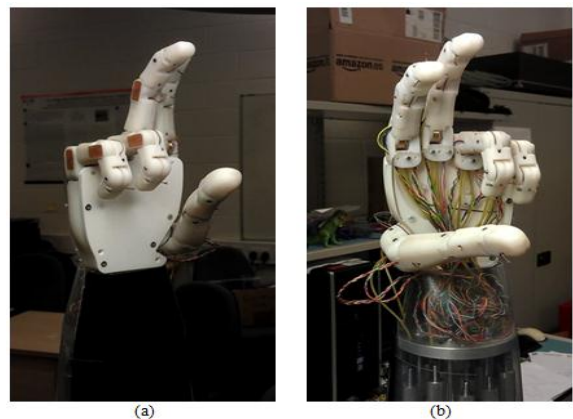
Figure 18: Ambidextrous hand, (a) is right mode and (b) is left model

Further developments should focus on increasing the range of movements by implementing the wrist rotation. The number of degree of freedom of the thumb should be increased to perform ambidextrous movements. Finally, testing the ability to grasp and lift different objects would complete the mechanical overview.

REFERENCES

[1] B.D. Darnall, "Self-Delivered Home-Based Mirror Therapy for Lower Limb Phantom Pain", *American Journal of Physical Medicine & Rehabilitation,* vol. 88, 2009, pp. 78-81.

[2] C.D. Murray, S. Pettifer, T. Howard, E. Patchick, F. Caillette, J. Murray, "Virtual Solutions to Phantom Problems: Using Immersive Virtual Reality to Treat Phantom Limb Pain" in *Amputation, Prosthesis Use, and Phantom Limb Pain*, ed. Craig Murray, 2010, pp. 175-196.

[3] T. Caires, M. Prywata, *"The Artificial Muscle-Operated (AMO) Arm"*, 2011. Available: http://www.robaid.com/bionics/brain-controlled-artificial-muscle-operated-amo-arm.htm.

[4] Y. Matsuoka, P. Afshar, and M. Oh, "On the design of robotic hands for brain–machine interface", *Neurosurg Focus 20,* vol. 20, 2006, pp. 1-9.

[5] X. Jiang, C. Xiong, R. Sun, and Y. Xiong "Characteristics of the Robotic Arm of a 9-DoF Upper Limb Rehabilitation Robot Powered by Pneumatic Muscles", *ICIRA 2010,* vol. LNAI 6425, 2010, pp. 463-474.

[6] Z. Li, *"Using robotic hand technology for the rehabilitation of recovering stroke patients with loss of hand power"*, Master of Science in Electrical Engineering Thesis, North Carolina State University, 2003.

[7] E. Akyürek, A. Dilly, F. Jourdan, Z. Liu, S. Chattoraj, I. Berruezo Juandeaburre, M. Heinrich, L. Paramonov, P. Turner, Stelarc, T. Kalganova, "Remote-Controlled Ambidextrous Robot Hand Concept", *Journal of Computer Technology and Application,* vol. 4, no. 4, 2013, pp. 569-574, in press.

[8] RSLSteeper, *Bebionic3*, 2012. Available: http://bebionic.com/the_hand/features.

[9] M. Stark, *The Natural Dexterous Hand*, 2011. Available: http://www.swisswuff.ch/tech/?p=427.

[10] A.M. Dollar and R.D. Howe, "The SDM Hand as a Prosthetic Terminal Device: A Feasibility Study", *Proc. IEEE International Conference on Rehabilitation Robotics, 2007*, pp. 978-983.

[11] A.D. Deshpande, Z. Xu, M.J. Vande Weghe, B.H. Brown, J. Ko, L.Y. Chang, D.D Wilkinson, S.M. Bidic, and Y. Matsuoka, "Mechanisms of the Anatomically Correct Testbed (ACT) Hand", *IEEE/ASME Transactions on Mechatronics,* vol. 18, 2013, pp. 238-250.

[12] Shadow Robot Company Ltd, *"Shadow Dexterous Hand E1M3R, E1M3L"*, 2013. Available: http://www.shadowrobot.com/products/dexterous-hand/.

[13] European Community's 7th Framework Programme "*The DEXMART hand"*, 2012. Available: http://www.dexmart.eu/.

[14] Festo *Exo-hand*, 2012. Available: http://www.festo.com/cms/en_corp/12713.htm.

[15] T. Mouri, H. Kawasaki, K. Yoshikawa, J. Takai, and S. Ito, "Anthropomorphic Robot Hand: Gifu Hand III", *Proc. of Int. Conf. ICCAS*, 2002, pp. 1288-1293.

[16] Ishikawa Oku Laboratory, *"High-speed robot hand"*, 2009. Available: http://www.k2.t.u-tokyo.ac.jp/fusion/HighspeedHand/.

[17] P.H. Chappell, N. White, and A. Cranny, "Development of a lightweight and adaptable multiple-axis hand prosthesis", *Medical Engineering & Physics,* vol. 22, 2000, pp. 679-684.

[18] G. Stellin, C. Cipriani, F. Zaccone, M.C. Carrozza, C. Laschi, and P. Dario, "Design of an anthropomorphic dexterous hand for a 2-years-old humanoid : ongoing work", *Proc. RoManSy, Tokyo, Japan, 2008*.

[19] Humanoid robotic portal, *The best five anthropomorphic robotic hands/arms*, 2012. Available: http://mindtrans.narod.ru/hands/hands.htm.

[20] E. Kelasidi, G. Andrikopoulos, G. Nikolakopoulos, and S. Manesis, "A Survey on Pneumatic Muscle Actuators Modeling", *Journal of Energy and Power Engineering,* vol. 6, 2012, pp. 1442-1452.

[21] Z. Varga and M. Moučka, "Mechanics of pneumatic artificial muscle", *Journal of applied science in the thermodynamics and fluid mechanics,* vol. 3, no. 4, 2009.

[22] Y. Honda, F. Miyazaki and A. Nishikawa, "Control of pneumatic five-fingered robot hand using antagonistic muscle ratio and antagonistic muscle activity", *Proc. 3rd IEEE RAS & EMBS International Conference on Biomedical Robotics and Biomechatronics*, 2010, pp. 337-342.

[23] Shadow Robot Company Ltd, *"Shadow Dexterous Hand E1P1R, E1P1L",* 2013. Available at: http://www.shadowrobot.com/products/dexterous-hand/.

[24] J.L. Sancho-Bru, A. Pérez-González, M. Vergara, D.J. Giurintano, "A 3D Biomechanical Model of the Hand for Power Grip", *Journal of Biomechanical engineering,* vol. 125, 2001, pp. 78-83.

[25] M. Grebenstein, A. Albu-Schäffer, T. Bahls, M. Chalon, O. Eiberger, W. Friedl, R. Gruber, U. Hagn, R. Haslinger, H. Höppner, S. Jörg, M. Nickl, A. Nothhelfer, F. Petit, B. Pleintinger, J. Reil, N. Seitz, T. Wimböck, S. Wolf, T. Wüsthoff, and G. Hirzinger, "The DLR Hand Arm System", *IEEE International Conference on Robotics and Automation (ICRA), 2011*, pp. 3175-3182.

[26] K.C. Wickramatunge and T. Leephakpreeda, "Study on mechanical behaviors of pneumatic artificial muscle", *International Journal of Engineering Science,* vol. 48, 2009, pp. 188-198.

[27] C.P. Chou, B.Hannaford, "Measurement and Modelling of McKibben Pneumatic Artificial Muscles", *IEEE Transactions on Robotics and Automation,* vol. 12, no. 1, 1996, pp. 90-102.

[28] C.S. Lovchik and M.A. Diftler (1999) "The Robonaut Hand: A Dexterous Robot Hand For Space", *Proc. IEEE International Conference on Robotics & Automation,* vol. 2, pp. 907-912.

[29] S. Kawamura, H. Kino, and C. Won, "High-speed manipulation by using wire-driven robots" in *Robotica,* ed. Cambridge University Press,United Kingdom, vol.18, 2000, pp. 13-21.

[30] H. Hu, J. Li, Z. Xie, B. Wang, H. Liu, and G. Hirzinger, "A robot arm/hand teleoperation system with telepresence and shared control", *Proceeding of the 2005 IEEE/ASME International Conference on Advanced Intelligent Mechatronics, 2005*, pp. 1312-1317.

[31] I. Yamano and T. Maeno, "Five-fingered Robot Hand using Ultrasonic Motors and Elastic Elements", Proceeding of the 2005 *International Conference on Robotics and Automation,* 2005, pp. 2673-2678.

[32] Meka, *H2 Compliant Hand, 2009*. Available at: http://mekabot.com/products/compliant-hand/.

[33] C.H. Kuo and C.T. Chen "Development of Tendon Based Dexterous Robot Hand" in *Advances in Robot Manipulators*, ed. Ernest Hall, 2010, pp. 255-266.

[34] Elumotion Ltd, *Elu2 hand, 2010*. Available at: http://www.elumotion.com/Elu2-hand.htm.

[35] Prensilia Srl, *The EH1 Milano Hand, 2010*. Available at: http://www.prensilia.com/index.php?q=en/node/41.

[36] D.D. Wilkinson, M. Vande Weghe, Y. Matsuoka, "An Extensor Mechanism for an Anatomical Robotic Hand", *Proc. IEEE International Conference on Robotics and Automation,* vol. 1, 2003, pp. 238-243.

[37] A.M. Zaid, M.A. Yaqub, M.R. Arshad, and M.S. Wahab, "UTHM Hand: Mechanics Behind The Dexterous Anthropomorphic Hand", *World Academy of Science, Engineering and Technology,* vol. 50, 2011, pp. 150-154.

[38] P.J. Kyberd, C. Light, P.H. Chappell, J.M. Nightingale, D. Whatley, and M. Evans, "The design of anthropomorphic prosthetic hands: A study of the Southampton Hand", *Robotica,* vol. 19, 2011, pp. 593-600.

[39] L. Biagotti, F. Lotti, C. Melchiorri, and G. Vassura, "Mechatronic Design of Innovative Fingers for Anthropomorphic Robot Hands", *Proc. IEEE International Conference on Robotics and Automation,* vol. 3, 2003, pp. 3187-3192.

[40] S. Boudoua, F. Hamerlain, and M. Hamerlain, "Neuro Sliding Mode Based Chatter Free Control for an Artificial Muscles Robot Arm", *International Joint Conference on Neural Networks (IJCNN), 2010*, pp. 1-7.

[41] K.K. Ahn and N.H.T. Chau, "Intelligent Phase Plane Switching Control of a Pneumatic Muscle Robot Arm with Magneto-Rheological Brake", *Journal of Mechanical Science and Technology,* vol. 21, 2007, pp. 1196-1206.

[42] F. Lotti, P. Tiezzi, G. Vasura, L. Biagotti, G. Palli, and C. Melchiorri, "Development of UB Hand 3: Early Results", *Proceedings of the 2005 IEEE International Conference on Robotics and Automation,* 2005, pp. 4488-4493.

[43] E. Akyürek, T. Kalganova, M. Mukhtar, L. Steele, M Simko, A Nimmo, L. Kavanagh, L Paramonov, A Huynh and Stelarc "A novel design of low cost 3D printed ambidextrous finger designed for an ambidextrous robotic hand", Robotics and Computer-Integrated Manufacturing, Elsevier Publisher. (Under Review)

[44] Chao, E.Y.S., An, K., Cooney, W.P. and Linscheid, R., *Biomechanics of the Hand*, Teaneck, NJ. USA: World Scientific Publishing Co. Pte. Ltd., 1989, pp. 5-75.

[45] J. R. Napier: The prehensile movements of the human hand, Journal of Bone and Joint Surgery, 38B (4): 902-913. 1956.

[46] Venkataraman, S.T. and Iderall, T., Dexterous Robot Hands, New York, NY: Springer-Verlag New York Inc., 1990, pp. 136-149.

[47] J. Hollerbach, Workshop on the Design and Control of Dexterous Hands, A.I. Memo 661, A.I. Laboratory, MIT, Cambridge, MA, 1982.

[48] A. Okamura, N. Smaby, M.R. Cutkosky, "An overview of dexterous manipulation," in Proc. 2000 International Conf. Robotics and Automation, 2000, pp. 255-262.

[49] Raymond R. Ma and Aaron M. Dollar, "On Dexterity and Dexterous Manipulation", The 15th International Conference on Advanced Robotics, Tallinn University of Technology, Tallinn, Estonia, June 20-23, 2011.

[50] Ortiz-Catalan M, Sander N, Kristoffersen MB, Håkansson B and Brånemark R (2014) Treatment of phantom limb pain (PLP) based on augmented reality and gaming controlled by myoelectric pattern recognition: a case study of a chronic PLP patient. *Front. Neurosci.* **8**:24. doi: 10.3389/fnins.2014.00024.

[51] Development and Application of a Gel Actuator for the Design of a Humanoid Robotic Finger Danielle Castley, Dr. Paul Oh *Mechanical Engineering and Mechanics, Drexel University,* 978-1-61284-481-7/11/2011 IEEE.

[52] Pain Relief Foundation, "Phantom Limb Pain"
http://www.painrelieffoundation.org.uk/docs/painseries%20-%20plp.pdf.

[53] K.Ramchandran and J.Hauser, "Phantom Limb Pain", End of life/ Palliative Education Resource Centre, Medical college of Wisconsin
http://www.eperc.mcw.edu/EPERC/FastFactsIndex/ff_212.htm.

[54] S.Shirafuji, S.Ikemoto and K.Hosoda"Design of An Anthropomorphic Tendon-Driven Robotic Finger", Proceedings of the 2012 IEEE International Conference on Robotics and Biomimetics December 11-14, 2012, Guangzhou, China.

[55] I.Yamano, K.Takemura and T.Maeno, "Development of a Robot Finger for Five-fingered Hand using Ultrasonic Motors", Proceedings of the 2003 IEEE/RSJ Intl. Conference on Intelligent Robots and Systems Las Vegas, Nevada · October 2003.

[56] Q.Yu, Y.Liu, B.Li andW.Zhou, "Introduction of a unique robotic hand: SIA- I Hand", Proceedings of the 8th World Congl'ess on Intelligent Control and Automation July 6-9 2010, Jinan, China

Emre Akyürek, successfully defended his PhD thesis title 'Remote-controlled Ambidextrous Robot Hand actuated by Pneumatic Muscles: from Feasibility Study to Design and Control Algorithms' at a viva held in October 2014, Brunel University, London.

Tatiana Kalganova, Senior Lecturer in Intelligent Systems at Brunel University, London. She obtained her PhD from Napier University, Research-engineer degree and Msc from Belarusian State University of Informatics and Radio-electronics, Minsk, Belarus. She has published number of journal, and conference papers. Her research interests include Artificial Intelligence, Evolutionary Design and Optimisation, Evolvable hardware, Modelling and optimisation of Large Systems, Operational research, Robotics and Swarm optimisation.

Mashood Mukhtar, received his Master of Engineering (M.Eng) degree from Queen Mary, University of London in 2011. He obtained Master of Business and Administration (MBA) in Finance from University of Gloucestershire in 2013. He is currently pursuing PhD with the department of Electronic and Computer Engineering, Brunel University, London. His research interests include Artificial Intelligence and Humanoid Robot.

Leonid Paramonov, is currently a Postdoctoral research fellow at Norwegian University of Science and Technology, Trondheim, Norway. He obtained his PhD from Brunel University, London.

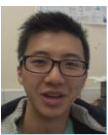**Luke Steele,** received his Master of Engineering (M.Eng) degree from Brunel University, London in 2013.

Michal Simko, received his Master of Engineering (M.Eng) degree from Brunel University, London in 2013.

Luke Kavanagh, received his Master of Engineering (M.Eng) degree from Brunel University, London in 2013.

Alisdair Nimmo, received his Master of Engineering (M.Eng) degree from Brunel University, London in 2013.

Anthony Huynh, received his Master of Engineering (M.Eng) degree from Brunel University, London in 2013.

Stelarc, is a performance artist, distinguished research fellow, Director Alternate Anatomies Lab, School of Design & Art, Curtin University Perth. In 2000 he was awarded an Honorary Degree of Laws by Monash University.